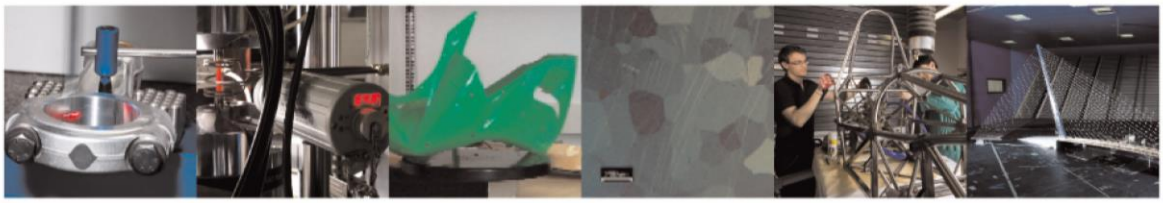

Laser surface structuring affects polymer deposition, coating homogeneity, and degradation rate of Mg alloys

Demir, Ali Gökhan; Taketa, Thiago B.; Tolouei, Ranna; Furlan, Valentina; Paternoster, Carlo; Beppu, Marisa M.; Mantovani, Diego; Previtali, Barbara

This is a post-peer-review, pre-copyedit version of an article published in MATERIALS LETTERS. The final authenticated version is available online at:
http://dx.doi.org/10.1016/j.matlet.2015.07.159

DIPARTIMENTO DI MECCANICA ■ POLITECNICO DI MILANO
via G. La Masa, 1 ■ 20156 Milano ■ EMAIL (PEC): pecmecc@cert.polimi.it
http://www.mecc.polimi.it
Rev. 0

Laser surface structuring affects polymer deposition, coating homogeneity, and degradation rate of Mg alloys

Ali Gökhan Demir[1], Thiago B. Taketa[2], Ranna Tolouei[3], Valentina Furlan[1], Carlo Paternoster[3], Marisa M. Beppu[2], Diego Mantovani[3], Barbara Previtali[1*]

[1] Department of Mechanical Engineering, Politecnico di Milano, Via La Masa 1, 20156 Milan, Italy

[2] School of Chemical Engineering, University of Campinas–UNICAMP, Av. Albert Einstein, 500, 13083-852, Campinas - SP, Brazil

[3] Lab. for Biomaterials and Bioengineering, Laval University, Quebec City, Canada.

*Corresponding author: barbara.previtali@polimi.it

Abstract

In the current work, a coating system consisted of a laser-structured surface, a thin layer primer and a polymeric coating to improve degradation behaviour of biocompatible and biodegradable Mg alloy is presented. The laser structuring allowed modification of surface topography as well as controlling the wettability of surface. The cellulose acetate primer provided protection from in-process degradation of samples during the successive layer-by-layer (LbL) coating process, where alternate layers of chitosan and carboxymethyl cellulose were applied. The results revealed that the laser structured surface plays an important role on the developed coating structure and final corrosion rate. Lowest corrosion rate among the coated samples (1.15 $cm \cdot yr^{-1}$) was measured for the most hydrophilic laser-treated surface, corresponding to almost 16% reduction compared to the as-received samples.

Keywords: Biodegradable metals; layer-by-layer coating; laser surface structuring

1. Introduction

Magnesium (Mg) alloys are highly attractive for biomedical applications and they provide a new insight for clinical applications in dentistry, orthopaedic, cardiac and vascular implants [1]. However, the high corrosion rate of Mg in physiological media prevents its widespread use for biomedical purposes [2]. The degradation pattern and corrosion rate should allow matching the optimal expected duration of implantation before the implant loses its functionality. Recently, biocompatible and biodegradable polymeric coatings are considered potential candidates for surface modification of biometals [3].

The layer-by-layer (LbL) technique is a simple and versatile way to assembly thin films on different kind of substrates, usually by alternating physisorption of oppositely charged polyelectrolytes [4]. Fabrication

of nanostructured films built up by polyelectrolyte multilayers of chitosan (CHI) as a positively charged polysaccharide while carboxymethyl cellulose (CMC) as a negatively charged one would be a great interest for such an application.

The use of laser surface treatments has been proposed on Mg alloys for their use in structural applications [5-7]. In most of these treatments continuous wave laser were used for surface remelting on a large depth extent, refining the alloy microstructure and generating intermetallic phases near the surface. Laser surface treatment can be also applied on a superficial layer to change surface topography, hence surface wettability [8]. For example, the use of pulsed lasers allow material interaction limited to nm-μm region depending on the pulse duration [9]. The process shows great flexibility in types of topographical and chemical modifications. The laser surface structuring can be used for surface preparation of a metal/polymer interface, as demonstrated for structural applications [10]. Despite its high potential, the use of laser surface treatment for enhancing the coating performance on a biomedical implant has not yet been explored.

In this work, the technology of LbL deposition of CHI/CMC in solution was used to investigate a corrosion-protective coating on Mg alloy (AZ31) with different laser-structured surfaces. The corrosion rate of the different surface structure-coating conditions was assessed to evaluate the feasibility and efficiency of the proposed solution for biodegradable implants.

2. Materials and methods

Cold rolled, 0.4 mm-thick AZ31 magnesium alloy sheets were selected for this study. The chosen alloy is among the most commercially available with corrosion properties much lower than other Mg alloys including rare-earth elements [13]. Laser surface structuring was performed with ns-pulsed fibre laser system and a scanning head in ambient atmosphere. Surface re-melting was employed with fluence levels of F=1-4 $J \cdot cm^{-2}$ to change the surface roughness [14]. Topography of the as-received condition (hereafter referred to as “plain”, Fig. 1) and two series of laser structured samples, “polished” and “worms”, was observed with focus variation microscopy (Alicona InfiniteFocus). A ring/plate tensiometer (Lauda Te 3) was used to measure the contact angle (θ).

The multilayer made by LbL deposition is composed by a primer of cellulose acetate (CA) and alternate layers of carboxymethyl cellulose (CMC) and chitosan (CHI). LbL was selected as it provided nm to μm thicknesses [15-17], and coating complex microstructured surfaces in a conformable way [18]. The used

primer layer allowed protection of the Mg alloy substrate from in-process degradation during the LbL dip coating phase. The primer was prepared by dissolving cellulose acetate (M_n≈30000, Sigma Aldrich) in acetone to 5 $g \cdot L^{-1}$. Spin coating was used to apply the coating on the plain and laser structured substrates using 200 µL of solution per sample. The substrates were rotated at 2000 rpm for 60 s, then the solvent was evaporated. For the LbL coating assembly, chitosan (low molecular weight, 75-85% deacetylate, Sigma Aldrich) was dispersed in Milli-Q water, followed by addition of 0.1 $mol \cdot L^{-1}$ acetic acid solution to reach 1 $g \cdot L^{-1}$ concentration. CMC (average M_w≈700,000, 0.9 carboxymethyl groups per anhydroglucose unit, Sigma Aldrich) was dissolved to 1 $g \cdot L^{-1}$ in Milli-Q water. The pH of CHI and CMC solutions was adjusted to 6.0 using 1 $mol \cdot L^{-1}$ NaOH or HCl solution whenever needed. Alternate layers of chitosan and CMC were built by immersing the primer coated substrate in CMC and CHI solutions for 2 min. Each layer was followed by one immersion in Milli-Q water (pH 6.0) for 30 s. Three bilayers of CMC/chitosan were applied on all substrates, and the polycation was set as the top layer. Samples were dried with N_2. Coating morphology was measured with tactile surface profilometry (KLA Tencor P-16+) using a 2 µm radius stylus tip at 60 degrees and 2 mg applied force. The coating thickness was assessed as the height step from the coating surface to the substrate. Fourier transform infrared (FTIR) spectroscopy in transmission mode was used to determine the functional groups of the coatings. X-ray photoelectron spectroscopy (XPS) was used to assess the surface chemistry of samples before and after the LbL coating. In vitro Static immersion test was performed according to *ASTM NACE/ASTMG31-12a*. Each specimen was separately suspended in 85 mL of phosphate buffer saline (PBS) solution and incubated in a controlled atmosphere ($T_{incubator}$ = 37.0 ± 1 °C, $p_{rel.\ CO2}$ = 5 %, 90% humidity) for 14 days. Solutions were changed every three days in order to maintain the pH at 7.4. At the end of the test, the degraded layers of the samples were removed by physical cleaning and rinsing in a sonicated bath of pure water, rinsed with distilled water and ethanol, dried and weighted. The degradation rate (DR) was determined based on the weight loss according to ASTM G31 standard. For each test combination, three replications were tested. Atomic absorption spectrometry (AAS) was employed to measure the release of Mg^{2+} ions in the test solution.

3. Results

SEM images of coated and uncoated sample surfaces are shown in Fig. 1. Different laser treatments as compared to plain sample surface induced a variety of surface morphology and wetting behavior, as

mentioned elsewhere [14]. Samples in the "polished" condition have generally a smoother surface and less defects than plain samples; furthermore they showed increased water contact angle (θ= 69±5º) compared to the plain condition. On the other side, the "worms" laser-treated surfaces showed a hydrophilic behaviour (θ=21±1º) together with a higher roughness value (R_a=1.07 µm). Demir *et al* [14] reported that worms surface type could be a potential treatment to enhance deposition of a polymeric coating over Mg-based alloys. This surface treatment reduced contact angle without any surface damage or excessive oxidation [19]. Table 1 reports the main properties of the surface types before and after coating application. After LbL deposition, a porous coating was obtained for all the surfaces with different laser treatments. The synergy between surface topography and wetting behaviour of laser-modified surfaces had an effect on the compactness (density) and structure of the LbL coating, as observed by SEM. LbL coating over worms sample appears to be more compact with a smaller pore size while the coating on polished sample is loosely packed. These results clearly show that laser structuring of the surface enhance adsorption of biomolecules and results in a more effective barrier for Mg substrates.

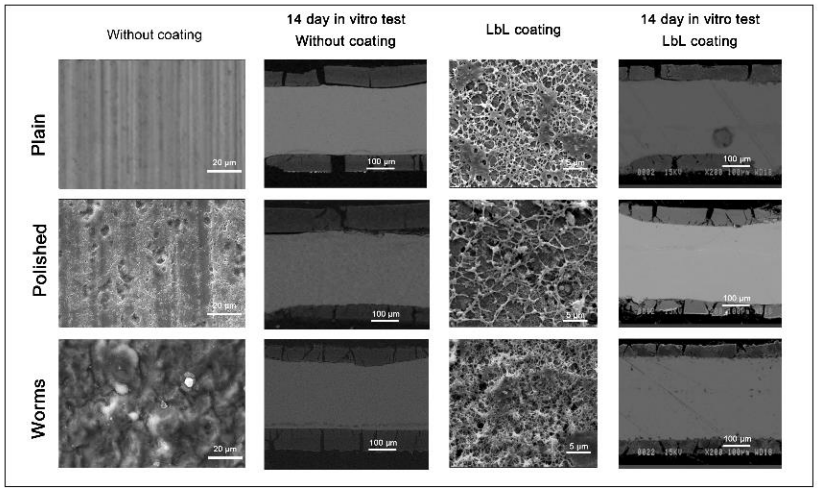

Figure 1.

Table 1.

XPS spectra of Mg-samples before and after LbL coating deposition displayed Mg, C and O peaks. The high C-content of uncoated samples could be attributed to environmental contaminations. After formation of LbL coating, presence of nitrogen can be attributed to the existence of amino groups of chitosan molecules over the surface. As indicated in Fig. 2.a, nitrogen amount is higher for worms in comparison with polished surface type. The observed high N-content for worms surface type is consistent with the

microscopic observation evidencing a more homogeneous coverage of the surface by the deposited LbL coating. Presence of the underlying metallic substrate (Mg) in spectra of coated samples could be attributed to inhomogeneity of the LbL coating. Moreover, the higher Mg-content for the polished surface could also indicate a thinner coating.

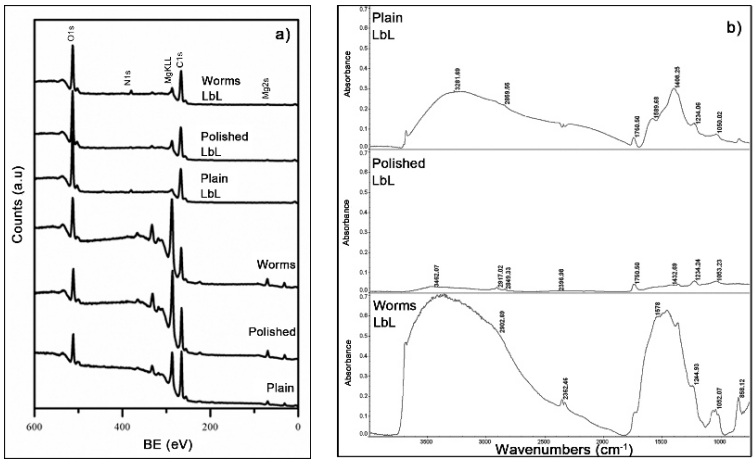

Figure 2.

The infrared spectrum of the CA-(CMC/CHI) multilayers is characterized by bands at 1050-1060 cm^{-1} (COO stretching in CMC and CA), 1234-1239 cm^{-1} (C–O stretch in CA), 1440 cm^{-1} (–CH_2 scissoring in CA and CMC), 1589 cm^{-1} (N–H stretching in CHI), 1755 cm^{-1} (C=O stretch in CMC and CA), 2854-2964 cm^{-1} (C–H stretch) and 3350 cm^{-1} (stretching of OH group), as shown in Fig. 2.b. Worms and plain samples after LbL coating deposition presented a stronger absorption along the spectra than polished samples. The coated samples showed notable reduction in Mg ion release, especially in the initial phase (see Fig. 3). The average corrosion rates of laser-treated samples with and without coatings are shown in Table 1. For all the conditions, the presence of the coating is responsible for a reduction in degradation rate. In particular, worms surface type with coating showed the slowest degradation rate of 1.15 mm y^{-1}, while the untreated and uncoated Mg samples showed a degradation rate of 1.37 mm y^{-1}. Sample SEM cross sections after 14 days of test are shown in Fig. 1. SEM analysis of sample surfaces showed that degradation of magnesium in PBS solution formed an inhomogeneous and thick layer of phosphate-based product. The thickness of the degradation product layers is generally non-uniform, but it is generally lower for coated ones. These results are in accordance with the average corrosion rate data. A thinner layer of degradation products concurrent with a lower amount of Mg ion released into the solution results in a slower degradation rate for the coated worms sample. The moderate degradation behaviour of worms

coated sample might be attributed to a denser polymeric barrier over the surface, which reduces the exposure of the metallic substrate to the test solution. Furthermore, the porous nature of LbL coating is a relevant parameter affecting Mg degradation rate: in fact Conceicao *et al.* [20] reported that a porous poly(ether imide) coating over a metallic substrate is responsible for a lower degradation rate than a denser one, because in the former case hydrogen is released without excessively damaging the coating and the interface.

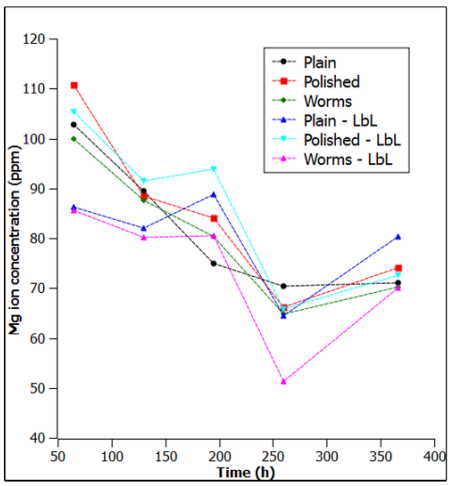

Figure 3.

In addition to role of the coating stability, the degradation process of the Mg alloy is also affected by solution composition, surface morphology and chemistry as well as microstructure [6, 21, 22]. In particular, the polished samples exhibit lower average roughness though a porous surface (Fig. 1). The presence of holes and cavities increases the local pH, triggering a degradation phenomenon run mainly by pitting [23]. Despite its high surface roughness, the "worms" type shows more homogenous topography without pores or cavities that could trigger pitting phenomena, which exhibits a more stable surface from the chemical point of view [23, 24]. Local instabilities may also set up after localized degradation phenomena (LbL coating degradation) and generate subsequent pitting. The increase in Mg ion release of plain-LbL samples (maximum after 360 h) is expected to be caused by this fact. Overall, the presence of the polymeric/polysaccharide coating has a levelling effect on the degradation of the material (more constant Mg ion release), leading to a decrease in the corrosion rate [25].

4. Conclusions

The present study proposed a polymeric coating procedure for Mg-based implants through a sequence of laser structuring, primer and LbL polysaccharide coating, aimed at controlling the degradation rate. The

structure of multilayer coating is strongly affected by the underlying laser treated surface. More specifically, the homogeneity of coating can be attributed to wettability of the surface, which is affected by surface texture. However, even the most porous layer has an effect on the degradation behaviour of Mg. After 14 days of immersion, the CHI/CMC layer totally disappears and a layer of degraded products forms on the surface of the immersed samples. The results depict that the proposed system is highly promising for tailoring the degradation behaviour of Mg-based implants by changing surface structure and coating conditions, to achieve a desired degradation rate for the destined application.

Acknowledgments

This project was partially financed by São Paulo Research Foundation (grant no. 2013/05135-1 FAPESP, MMB) and CNPq (MMB), the Natural Science and Engineering Research Council of Canada (DM) Quebec Ministry of International Relations and Foreigner Affairs Italian Ministry (project no. 08.205 to DM and BP), and Politecnico di Milano (BP).

References

1. Witte F. The history of biodegradable magnesium implants: A review. Acta Biomater. 2010; 6(5):1680-92.
2. Zheng YF, Gu XN, Witte F. Biodegradable metals. Mat Sci Eng R. 2014;77(0):1-34.
3. Babu R, O'Connor K, Seeram R. Current progress on bio-based polymers and their future trends. Prog Biomater. 2013;2(8):1-16.
4. Decher G. Fuzzy Nanoassemblies: Toward Layered Polymeric Multicomposites. Science. 1997;277(5330):1232-37.
5. Abbas G, Liu Z, Skeldon P. Corrosion behaviour of laser-melted magnesium alloys. Appl Surf Sci 2005; 247:347–53
6. Taltavull C, Torres B., López AJ, Rodrigo P, Rams J. Novel laser surface treatments on AZ91 magnesium alloy. Surf Coat Tech. 2013;222:118–27
7. Taltavull C, Torres B, Lopez AJ, Rodrigo P, Otero E, Atrens A, Rams J, Corrosion behaviour of laser surface melted magnesium alloy AZ91D. Mater Design. 2014;57: 40–50
8. Kietzig A-M, Hatzikiriakos SG, Englezos P. Patterned Superhydrophobic Metallic Surfaces. Langmuir. 2009; 25:4821- 27
9. Chichkov BN, Momma C, Nolte S, von Alvensleben F, Tünnermann A. Femtosecond, picosecond and nanosecond laser ablation of solids. Appl. Phys. A. 1996;63:109-15
10. Spadaro C, Sunseri C, Dispenza C, Laser surface treatments for adhesion improvement of aluminium alloys structural joints. Radiat. Phys. Chem. 2007;76:1441–46.
11. Maressa P, Anodio L, Bernasconi A, Demir AG, Previtali B. Effect of Surface Texture on the Adhesion Performance of Laser Treated Ti6Al4V Alloy. J Adhesion. 2015;91(7): 518-37
12. Heckert A, Zaeh MF, Laser surface pre-treatment of aluminum for hybrid joints with glass fiber reinforced thermoplastics. J Laser App. 2015; 27: S29005(5pp)
13. Zheng YF, Gu XN, Witte F. Biodegradable metals, Mat Sci Eng R 77 2010;15(2):96–103
14. Demir AG, Furlan V, Lecis N, Previtali B. Laser surface structuring of AZ31 Mg alloy for controlled wettability. Biointerphases. 2014;9(2):29009 (10pp).
15. Shiratori SS, Ito T, Yamada T. Automatic film formation system for ultra-thin organic/inorganic hetero-structure by mass-controlled layer-by-layer sequential adsorption method with ‘nm’ scale accuracy. Colloid Surfaces A. 2002;198–200(0):415-23.
16. Lvov Y, Ariga K, Onda M, Ichinose I, Kunitake T. A careful examination of the adsorption step in the alternate layer-by-layer assembly of linear polyanion and polycation. Colloid Surfaces A. 1999;146(1–3):337-46.

17. Dubas ST, Schlenoff JB. Factors Controlling the Growth of Polyelectrolyte Multilayers. Macromolecules. 1999;32(24):8153-60.
18. Polak R, Crouzier T, Lim RM, Ribbeck K, Beppu MM, Pitombo RNM et al. Sugar-Mediated Disassembly of Mucin/Lectin Multilayers and Their Use as pH-Tolerant, On-Demand Sacrificial Layers. Biomacromolecules. 2014;15(8):3093-98.
19. Furlan V, Demir AG, Previtali B. Micro and sub-micron surface structuring of AZ31 by laser re-melting and dimpling. Opt Laser Technol. 2015;75:164-172
20. Conceicao TF, Scharnagla N, Blawerta C, Dietzela W, Kainer KU. Corrosion protection of magnesium alloy AZ31 sheets by spin coating process with poly (ether imide)[PEI]. Corros Sci. 2010;52(6):2066-79.
21. Xin Y, Hu T, Chu PK. In vitro studies of biomedical magnesium alloys in a simulated physiological environment: A review. Acta Biomater. 2011;7:1452-59.
22. Song G-L. Corrosion electrochemistry of magnesium (Mg) and its alloys. In: Song G-L editor. Corrosion of Magnesium Alloys, Cambridge: Woodhead Publishing; p. 3-65
23. Walter R, Bobby Kannan M, He Y, Sandham A. Effect of surface roughness on the in vitro degradation behaviour of a biodegradable magnesium-based alloy. Appl Surf Sci. 2013, 279:343-48
24. Walter R, Bobby Kannan M, Influence of surface roughness on the corrosion behaviour of magnesium alloy. Mater Design. 2011, 32:2350-54
25. Ostrowski N, Lee B, Enick N, Carlson B, Kunjukunju S, Roy A, Kumta PN. Corrosion protection and improved cytocompatibility of biodegradable polymeric layer-by-layer coatings on AZ31 magnesium alloys. Acta Biomater. 2013, 9:8704-13

Figure Captions

Figure 1. SEM micrographs of different surface types with and without coating showing the surface morphology before coating application and cross sections after in vitro degradation test.

Figure 2. a) XPS spectra of the different surface types before and after LbL coating, b) FTIR spectra of the different surface types with LbL coating.

Figure 1. Mg ion release as a function of immersion time measured on different surface types with and without LbL coating.

Table 1. Main properties of different surface types with and without LbL coating.

	Non-coated			Coated		
Surface type	R_a [µm]	θ [°]	CR [mm.yr^{-1}]	R_a [µm]	Coat. thickness [µm]	CR [mm.yr^{-1}]
Plain	0.26±0.01	61±4	1.37±0.02	0.19±0.01	1.1	1.17±0.05
Polished	0.22±0.01	69±5	1.52±0.05	0.26±0.05	1.5	1.27±0.01
Worms	1.07±0.05	22±1	1.32±0.01	1.54±0.03	3.0	1.15±0.01